Dalton Transactions

Cite this: *Dalton Trans.*, 2012, **41**, 1938

www.rsc.org/dalton

PAPER

Synthesis, Cu(II) complexation, ^{64}Cu-labeling and biological evaluation of cross-bridged cyclam chelators with phosphonate pendant arms†

Riccardo Ferdani,[a] Dannon J. Stigers,[b] Ashley L. Fiamengo,[a] Lihui Wei,[a] Barbara T. Y. Li,[b] James A. Golen,[c] Arnold L. Rheingold,[d] Gary R. Weisman,*[b,e] Edward H. Wong*[b,f] and Carolyn J. Anderson*[a,g,h]

Received 15th September 2011, Accepted 1st November 2011
DOI: 10.1039/c1dt11743b

A new class of cross-bridged cyclam-based macrocycles featuring phosphonate pendant groups has been developed. 1,4,8,11-tetraazacyclotetradecane-1,8-di(methanephosphonic acid) (CB-TE2P, **1**) and 1,4,8,11-tetraazacyclotetradecane-1-(methanephosphonic acid)-8-(methanecarboxylic acid) (CB-TE1A1P, **2**) have been synthesized and have been shown to readily form neutral copper(II) complexes at room temperature as the corresponding dianions. Both complexes showed high kinetic inertness to demetallation and crystal structures confirmed complete encapsulation of copper(II) ion within each macrocycle's cleft-like structure. Unprecedented for cross-bridged cyclam derivatives, both CB-TE2P (**1**) and CB-TE1A1P (**2**) can be radiolabeled with ^{64}Cu at room temperature in less than 1 h with specific activities >1 mCi μg^{-1}. The *in vivo* behavior of both ^{64}Cu-CB-TE2P and ^{64}Cu-CB-TE1A1P were investigated through biodistribution studies using healthy male Lewis rats. Both new compounds showed rapid clearance with similar or lower accumulation in non-target organs/tissues when compared to other copper chelators including CB-TE2A, NOTA and Diamsar.

Introduction

The quest for an optimal bifunctional chelator (BFC) continues to be one major goal in the research and development of metal-based radiopharmaceuticals for clinical imaging and therapeutic applications. An ideal BFC should bind the targeted radiometal with high specificity, yield, and with alacrity. Further, the resulting complex should be both thermodynamically stable and, more importantly, kinetically inert to *in vivo* transchelation or trans-metallation processes. Copper-64 ($T_{1/2}$ = 12.7 h; β$^+$: 0.656 MeV, 17.8%; β$^-$: 0.573 MeV, 38.4%) is a promising radiometal with potential for applications in diagnostic imaging (positron emission tomography (PET)) and targeted radiotherapy.[1–3] It can also be produced in high yield and specific activity from a medical cyclotron.[4] Targeting ^{64}Cu(II), a variety of acyclic, macrocyclic, as well as macrobicyclic polyamine BFC's have been studied and reported.[2,5–10] Kinetic stability of Cu(II) complexes has been shown to be more predictive of *in vivo* stability than thermodynamic stability.[11] Macrocyclic chelators of Cu(II) such as TETA (1,4,8,11-tetraazacyclotetradecane-1,4,8,11-tetraacetic acid) demonstrated higher kinetic inertness and thus *in vivo* stability relative to acyclic chelators such as EDTA (ethylenediamine tetraacetic acid).[12,13] However, biodistribution and metabolism studies of ^{64}Cu-labeled TETA and TETA-biological molecule conjugates have revealed significant transchelation of ^{64}Cu to superoxide dismutase and metallothionein in liver and albumin in blood resulting in high background radioactivity.[14,15]

We have previously developed a dicarboxymethyl pendant-armed cyclam macrocycle featuring an ethylene cross-bridge, CB-TE2A (4,11-bis(carboxymethyl)-1,4,8,11-tetraazabicyclo[6.6.2]hexadecane; Fig. 1),[16,17] and shown that it possesses many of the desirable attributes to be an effective BFC for ^{64}Cu(II).‡ The resulting radiolabeled complex[18] has been found to exhibit significantly improved *in vivo* behavior compared to non-cross-bridged analogs like TETA.[15,17,19–21] We hypothesize that both its kinetic inertness to ^{64}Cu(II) loss and resistance to

[a]*Mallinckrodt Institute of Radiology, Washington University School of Medicine, St. Louis, Missouri, 63110, USA*
[b]*Department of Chemistry, University of New Hampshire, Durham, New Hampshire, 03824, USA*
[c]*Department of Chemistry and Biochemistry, University of Massachusetts, Dartmouth, North Dartmouth, Massachusetts, 02747, USA*
[d]*Department of Chemistry and Biochemistry, University of California, San Diego, La Jolla, California, 92093, USA*
[e]*E-mail: gary.weisman@unh.edu*
[f]*E-mail: ehw@unh.edu*
[g]*Department of Biochemistry and Molecular Biophysics; Department of Chemistry, Washington University, St. Louis, Missouri, 63110, USA*
[h]*Current address: Department of Radiology, University of Pittsburgh, Pittsburgh, PA 15219, USA. E-mail: andersoncj@upmc.edu*

† Electronic supplementary information (ESI) available: Details of HPLC purification of CB-TE1A1P (**2**), X-ray software employed; detailed energetic results for DFT calculations; and NMR spectra of ligand **2** and precursor **6**. CCDC reference number 843734. For ESI and crystallographic data in CIF or other electronic format see DOI: 10.1039/c1dt11743b

‡ In this paper ligand acronyms and numbers refer not only to the neutral species shown in Fig. 1 and elsewhere, but also to the various deprotonated forms that may complex metal cation, with net charge indicating ionization state of the ligand or ligand portion of any complex.

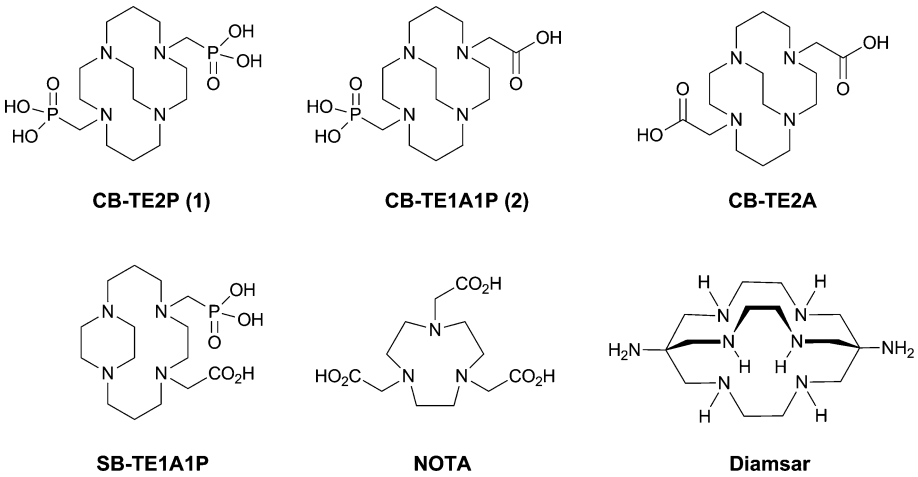

Fig. 1 Structures of ligands studied or discussed.

biological reduction contribute to these enhanced properties. CB-TE2A[9,17,20,22–25] and derivatives[26–29] have been successfully bioconjugated to targeting peptides and investigated by us and other research groups.

A less-than-optimal aspect of the useful BFC CB-TE2A lies in the rather sluggish radio-copper binding kinetics necessitating relatively harsh labeling conditions (95 °C heating for 1–1.5 h) which can handicap its bioconjugation to more fragile targeting moieties. To overcome this limitation, we have developed a second generation of cross-bridged chelators incorporating methanephosphonic acid pendant arms. A number of phosphonate pendant-armed tetraazamacrocyclic chelators have been studied previously.[30–46] Substitution of methanephosphonic acid pendant arms for acetic acid functional groups has resulted in complexes having higher selectivity for Cu(II) and an increased thermodynamic and kinetic stability.[47] Radiochemistry, *in vitro* and *in vivo* stability, and biodistribution studies were reported for ^{64}Cu-labeled cyclen derivatives having 2, 3 or 4 methanephosphonate pendant arms (DO2P, DO3P and DOTP, respectively).[48] Cu(II)-DO2P was found to have a very high formation constant (log$K$ = 28.7), while its ^{64}Cu-complex exhibited high *in vitro* stability in rat serum and a very rapid disappearance from the blood, liver and kidney. A higher bone uptake for ^{64}Cu-DO3P and ^{64}Cu-DOTP was observed, most likely due to the fact that methanephosphonate sidearms are known to have great affinity for the hydroxyapatite in the bone.[49–52] A side-bridged cyclam derivative with mixed phosphonate/acetate pendant arms, SB-TE1A1P (Fig. 1), has also been reported, though heating was still required for high ^{64}Cu-labeling yields.[53] A related side-bridged phosphonate BFC precursor has also been reported.[54]

Recently, we communicated in this journal the synthesis and characterization of the first methanephosphonic acid derivative of cross-bridged cyclam, CB-TE2P (1,4,8,11-tetraazacyclotetradecane-1,8-di(methanephosphonic acid), Fig. 1), its Cu(II) complex Cu-CB-TE2P, and ^{64}Cu(II) labeling and biodistribution studies.[55] Pleasingly, the anticipated acceleration of Cu(II) complexation was realized. However, the actual use of CB-TE2P as a BFC using conventional bioconjugation protocols is less straightforward. We have now prepared a mixed-armed variation, CB-TE1A1P (1,4,8,11-tetraazacyclotetradecane-1-(methanephosphonic acid)-8-(methanecarboxylic acid), Fig. 1), featuring both a methanephosphonic acid as well as a carboxymethyl pendant arm. We surmise that the former pendant arm will enhance the Cu(II) binding rate while the latter provides a scaffold to facilitate bioconjugation. In this report, we detail the synthesis and characterization of both CB-TE2P and CB-TE1A1P, and their respective copper(II) complexes, Cu-CB-TE2P and Cu-CB-TE1A1P.[56] Their ^{64}Cu-labeling along with biodistribution studies have also been carried out for comparison with other widely used BFC's including CB-TE2A, NOTA (1,4,7-triazacyclononane-1,4,7-triacetic acid), and Diamsar (1,8-diamino-3,6,10,13,16,19-hexaazabicyclo[6.6.6]icosane) (Fig. 1).

Results and discussion

Ligand synthesis and characterization

As previously communicated,[55] CB-TE2P (**1**) was synthesized in two steps from cross-bridged cyclam **3**[16] (Scheme 1(a)). **3** was first converted to bis-diethylphosphonate **4** by a variant of the Kabachnik–Fields three-component reaction[57–61] and this synthetic intermediate was then hydrolyzed to CB-TE2P. Thus, reaction of **3** with triethylphosphite and paraformaldehyde in anhydrous THF under nitrogen at room temperature for 4 days gave pure **4** in 94% yield after extractive workup. **4** was hydrolyzed in 6 M HCl under reflux for 24 h to give **1** in 64% yield as a hydrochloride after purification by ion exchange chromatography.

NMR spectroscopic results for this salt are similar to NMR spectra of previously studied di-inside-protonated salts of cross-bridged ligands[62] and are consistent with a C_2-symmetric diamond-lattice [2323]/[2323] conformation[16,63,64] for the bicyclic backbone in solution, which is the conformation that has been observed in the solid state for such cross-bridged salts.[62] In the ^{1}H NMR spectrum, every geminal pair of hydrogens is diastereotopic and anisochronous and exhibits the coupling patterns and coupling constants expected of an equatorial/axial pair of hydrogens in a diamond-lattice arrangement (see the Experimental for detailed interpretation and the ESI for spectra†). However, neither a related non-diamond-lattice [2233]/[2233] conformation, which differs from the former by a change in sign of the cross-bridge N–C–C–N torsion angle, nor a time-averaged dynamic mixture of these two conformations in solution can be rigorously

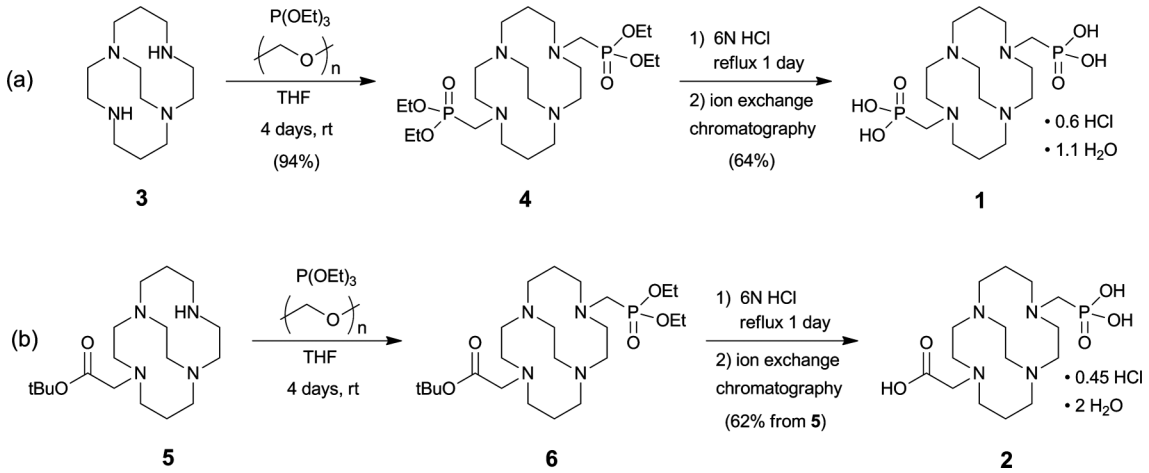

Scheme 1

excluded as possibilities. Nevertheless, we were surprised when an X-ray crystal structure of **1**·HCl·4H_2O (Fig. 2), reported in our preliminary communication, showed the ligand adopting a [2233]/[2233] conformation rather than the expected [2323]/[2323] diamond-lattice conformation. A possible explanation for this observation lies in the fact that net-positively-charged di-inside-protonated ligand possesses one phosphonic acid arm and one phosphonate arm and these are shown to be intramolecularly O–H···O hydrogen bonded (disordered) in the solid state. This conformation of the ligand backbone may be necessary in order to facilitate the appropriate arm-arm distance for the intramolecular H-bond. In aqueous solution, solvation of phosphonate arms would likely dominate over arm-arm intramolecular H-bonding, so the diamond-lattice backbone conformation may be favored in solution.

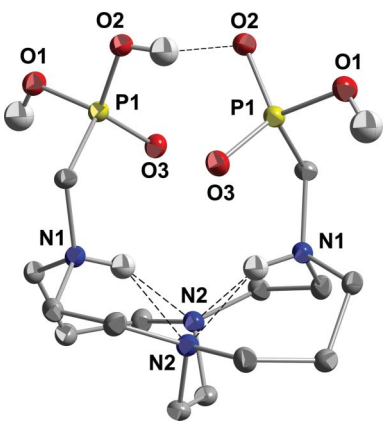

Fig. 2 X-ray structure of **1**·HCl·4H_2O (50% thermal ellipsoids for all non-hydrogen atoms). Intramolecular hydrogen bonds are shown as dashed lines. One of the two half-occupancy symmetry-related hydrogens on O2 has been removed for clarity so that the H-bond can be shown.

CB-TE1A1P (**2**) was synthesized similarly in two steps from the previously reported unsymmetrical synthetic intermediate CB-TE1A *tert*-butyl ester **5** (Scheme 1(b)).[19] **5** was reacted with triethylphosphite and paraformaldehyde in anhydrous THF for 4 days at room temperature to give, after an extractive workup, the corresponding phosphonate ester **6**, which was taken on to the next step without further purification. Hydrolysis of both the diethylphosphonate and *tert*-butyl carboxylic ester moieties of **6** was accomplished in refluxing 6 M HCl to give **2** in 62% overall (two step) yield from **5** as a hydrochloride salt after purification by ion exchange chromatography (Scheme 1(b)). This salt can be further purified if necessary by reversed-phase HPLC (C18; 0.1% TFA in H_2O/0.1% TFA in MeCN) to give **2** as a di-TFA salt. The detailed NMR characterization reported in the Experimental section is of **2**·2.5TFA. As was the case for the salt of **1**, the NMR spectroscopic results for **2**·2.5TFA are indicative of a di-inside-protonated species having a diamond-lattice [2323]/[2323] conformation in solution (see the Experimental for detailed interpretation and the ESI for spectra†). In the ^{1}H spectrum, each geminal pair of hydrogens is diastereotopic and anisochronous, exhibiting the characteristic coupling patterns consistent with the diamond-lattice [2323]/[2323] geometry, although neither the [2233]/[2233] nor a time average of the two can be excluded. Both the ^{1}H and ^{13}C{^{1}H} NMR spectra exhibit the expected ^{31}P couplings and point to the expected lack of symmetry. The ^{31}P{^{1}H} spectrum exhibits one signal.

Synthesis and characterization of copper(II) complexes of CB-TE2P and CB-TE1A1P

The Cu(II) complex of CB-TE2P was initially prepared from $CuCl_2$ and the ligand in refluxing methanol with the pH adjusted to 8 using aqueous NaOH. Subsequently, it was found that complexation in methanol was already complete in less than 5 min at ambient temperature. The blue complex has a d-d absorption maximum at λ_{max} (MeOH)/nm 639 (ε/dm^3 mol^{-1} cm^{-1} 35). Its cyclic voltammogram in 0.1 M aq. NaOAc exhibited a *quasi*-reversible reduction at –0.96 V (Ag/AgCl), typical of Cu(II) cross-bridged cyclam complexes. Its acid inertness was assayed under *pseudo* first-order conditions in 5 M HCl at 90 °C and found to have a half life of 3.8(1) h. While this is much less impressive than the 154 h previously reported for Cu-CB-TE2A, it is nonetheless significantly more inert than both Cu-DOTA and Cu-TETA which completely decomplexed within minutes.

As desired, the complexation of copper(II) by CB-TE1A1P also proceeded readily at room temperature even in acidic aqueous solution. The isolated dark-blue complex exhibited a carboxylate

stretching band at 1619 cm^{-1} in its IR spectrum and a d–d band maximum at 613 nm (ε/dm^3 mol^{-1} cm^{-1} 24) in its electronic spectrum. In contrast to previously reported cross-bridged cyclam copper(II) complexes including Cu-CB-TE2P, the electrochemical reduction of Cu-CB-TE1A1P has been found to be irreversible with a peak potential at around −1.0 V (Ag/AgCl) accompanied by a large copper stripping peak in the reverse scan. Acid inertness studies of the complex in 5 M HCl at 90 °C gave a half-life of 6.8(1) h which is comparable to Cu-CB-TE2P though both are significantly less acid-resistant than Cu-CB-TE2A (half-life = 154(6) h).

X-ray structures of Cu-CB-TE2P and Cu-CB-TE1A1P

The X-ray crystal structure of Cu-CB-TE2P[55] is shown in Fig. 3. Full envelopment of the cation within the ligand's N_4O_2 donor set results in a distorted octahedral coordination mode. Observed elongated bond lengths of 2.20 Å for N(4)–Cu(1) and 2.45 Å for Cu(1)–O(6) designate the expected Jahn–Teller distortion axis. Further, an N(1)–Cu(1)–N(3) bond angle of 174.8° confirms a good fit of the cation inside the chelator cavity. This can be compared to the 177.5° for the analogous angle in the Cu-CB-TE2A structure. Interestingly, here the ligand adopts a [2233]/[2233] conformation rather than the distorted diamond-lattice [2323]/[2323] conformation more commonly seen in reported Cu(II) complexes of cross-bridged cyclams, including Cu-CB-TE2A.[16,19,65–68] However, the [2233]/[2233] conformation has also been found in the structure of monoprotonated Cu-CB-TE2A (as a perchlorate salt)[11] and in a Cu(II) complex of the diamide analog of CB-TE2A.[69]

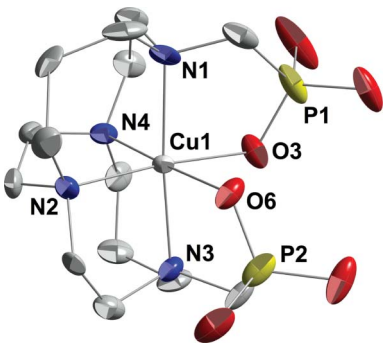

Fig. 3 X-ray structure of Cu-CB-TE2P (50% thermal ellipsoids for all non-hydrogen atoms). Only one of two independent complexes is shown. Both exhibit distorted octahedral coordination at Cu and have the same ligand conformation. Hydrogens, sodium and chloride ions, and solvent molecules have been removed for clarity.

The X-ray structure of Cu-CB-TE1A1P also has the expected full six-coordinate N_4O_2 envelopment of the cation with the methylphosphonate arm monoprotonated to give a charge-neutral complex overall (Fig. 4). The Jahn–Teller elongation here is found along the O(1)–Cu(1)–N(2) axis with the phosphonate Cu–O 2.544(3) Å and Cu–N 2.220(3) Å. In comparison, the Cu(1)–O(4) bond to the carboxylate oxygen is much shorter at 1.993(2) Å. It should be noted that each phosphonate P(O)OH moiety is hydrogen bonded to the P(O)OH of another complex in a dimeric structure, so it may be that the weaker phosphonate coordination and apparent Jahn–Teller elongation is partly a consequence

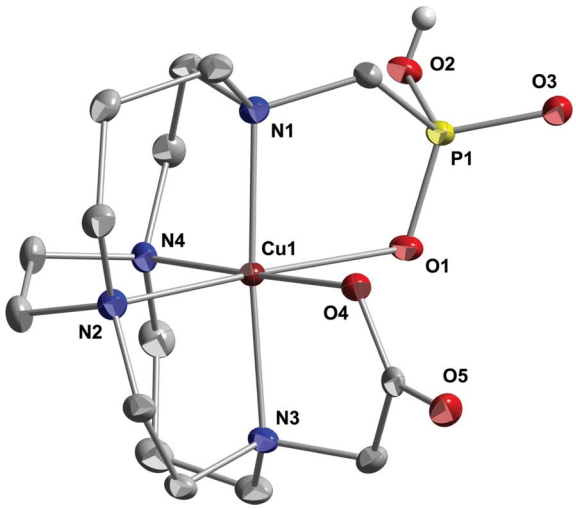

Fig. 4 X-ray structure of Cu-CB-TE1A1P (50% thermal ellipsoids for all non-hydrogen atoms). Hydrogens other than the phosphonate hydrogen and solvent molecules have been removed for clarity.

of this competing hydrogen bonding. An observed *exo* N(1)–Cu(1)–N(3) angle of 175.0(1)° indicates that the cation is slightly sunken into the ligand cleft. Again, the ligand here adopts the [2233]/[2233] conformation suggesting that methanephosphonate pendant arms, with their longer P–C and P–O bonds compared to the C–C and C–O bonds of acetate arms, may dictate this optimum cross-bridged cyclam conformation for Cu(II) binding. Alternatively, the conformations may be similar enough in energy that solvation or packing effects could determine the preference.

Significant bonding data for both complexes are listed for comparison in Table 1. To sum up the structural results, both CB-TE2P and CB-TE1A1P have been shown to readily form six-coordinate copper(II) complexes at ambient temperature resulting in full envelopment of the cation by the respective chelator. Each of these complexes adopts the more unusual [2233]/[2233] conformation in the solid state. Our assays of these products further confirmed that both should be sufficiently inert to acid

Table 1 Comparison of bond lengths and angles in Cu-CB-TE2P and Cu-CB-TE1A1P

Cu-CB-TE2P		Cu-CB-TE1A1P	
Bond distances in Å and bond angles in (°)			
Cu(1)–O(6)	2.450(5)	Cu(1)–O(1)	2.544(3)
Cu(1)–O(3)	1.998(5)	Cu(1)–O(4)	1.993(2)
Cu(1)–N(1)	2.087(6)	Cu(1)–N(1)	2.053(3)
Cu(1)–N(2)	2.035(7)	Cu(1)–N(2)	2.220 (3)
Cu(1)–N(3)	2.041(6)	Cu(1)–N(3)	2.078(3)
Cu(1)–N(4)	2.205(7)	Cu(1)–N(4)	2.032(3)
O(3)–Cu(1)–N(2)	174.4(2)	O(4)–Cu(1)–N(4)	178.5(1)
O(3)–Cu(1)–N(2)	88.8(2)	O(4)–Cu(1)–N(1)	92.4(1)
N(2)–Cu(1)–N(3)	85.6(3)	N(4)–Cu(1)–N(1)	86.3(1)
O(3)–Cu(1)–N(1)	87.5(2)	O(4)–Cu(1)–N(3)	83.5(1)
N(2)–Cu(1)–N(1)	98.1(3)	N(4)–Cu(1)–N(3)	97.9(1)
N(3)–Cu(1)–N(1)	174.8(3)	N(1)–Cu(1)–N(3)	175.0(1)
O(3)–Cu(1)–N(4)	94.5(2)	O(4)–Cu(1)–N(2)	93.1(1)
N(4)–Cu(1)–N(2)	86.2(3)	N(4)–Cu(1)–N(2)	86.3(1)
N(3)–Cu(1)–N(4)	99.7(2)	N(1)–Cu(1)–N(2)	99.1(1)
N(1)–Cu(1)–N(4)	84.3(2)	N(3)–Cu(1)–N(2)	83.9(1)

(Numbers in parentheses refer to estimated standard deviations)

decomplexation and resistant to reduction by common biological reductants.

Density Functional Theory (DFT) MO calculations on Cu-CB-TE2A, Cu-CB-TE2P and Cu-CB-TE1A1P

The structural results (*vide supra*) led us to investigate whether the preference of Cu-CB-TE2P and Cu-CB-TE1A1P for the [2233]/[2233] conformation over the more commonly observed [2323]/[2323] conformation observed in Cu-CB-TE2A and most other cross-bridged cyclam metal complexes is a result of fundamental geometric and electronic factors within each coordination complex, or whether the energies of the conformations are so similar that differences in solvation and packing might logically be determining solid-state conformation. While the conformational change is largely associated with the organic portion of the coordination complex, we felt that a molecular mechanics (force field) approach would not properly account for differences in copper coordination and so proceeded to carry out density functional theory (DFT) calculations (gas phase) on the [2233]/[2233] and [2323]/[2323] conformations of Cu-CB-TE2P, Cu-CB-TE1A1P and Cu-CB-TE2A using basis sets as large as practical considering the size of these coordination complexes. Two density functionals were employed, the very commonly used B3LYP[70–74] and the M06 functional of Truhlar,[75,76] which has been shown to give better results for metal complexes.[77] In each case, the all-electron 6-31G* basis set was employed and geometry optimization was carried out (E, kcal mol^{-1}). Furthermore, in each case a frequency calculation was carried out so that zero-point energy (ZPE) corrections could be made (E_{corr}, kcal mol^{-1}) and free energies (G, kcal mol^{-1} at 298 K) could be calculated. In the case of the M06 functional, single-point calculations at the M06/6-31+G**//M06/6-31G* level were also carried out for both conformations of all three complexes. The results (energies in kcal mol^{-1}) are summarized in Table 2.

Inspection of the relative (gas phase) ZPE-corrected energies and free energies in Table 2 show that the calculations using the more reliable M06 functional qualitatively reproduce the relative conformational energies implied by the crystallographic results. The M06/6-31G*//M06/6-31G* calculations show the [2233]/[2233] conformer to be more stable for CB-TE2P and CB-TE1A1P and the [2323]/[2323] conformer to be favored for CB-TE2A. The single point M06/6-31+G**//M06/6-31G* energy differences are not significantly different from the lower level basis E differences for Cu-CB-TE2P and Cu-CB-TE1A1P. The gap

Table 2 DFT energetic results for conformers of Cu-CB-TE2P, Cu-CB-TE1A1P, and Cu-CB-TE2A

Cu-CB-TE2P			
B3LYP/6-31G*//B3LYP/6-31G*:		Relative energies (kcal mol^{-1})	
Conformer	E	E_{corr}[a]	G (298 K)
[2233]/[2233]	0	0	0.18
[2323]/[2323]	0.49	0.01	0
M06/6-31G*//M06/6-31G*:		Relative energies (kcal mol^{-1})	
Conformer	E	E_{corr}[a]	G (298 K)
[2233]/[2233]	0	0	0
[2323]/[2323]	0.92	0.70	0.50
M06/6-31+G**//M06/6-31G*:		Relative energies (kcal mol^{-1})	
Conformer	E	E_{corr}[a]	G (298 K)
[2233]/[2233]	0	—	—
[2323]/[2323]	0.86	—	—
Cu-CB-TE1A1P			
B3LYP/6-31G*//B3LYP/6-31G*:		Relative energies (kcal mol^{-1})	
Conformer	E	E_{corr}[a]	G(298 K)
[2233]/[2233]	0.31	0.07	0.06
[2323]/[2323]	0	0	0
M06/6-31G*//M06/6-31G*:		Relative energies (kcal mol^{-1})	
Conformer	E	E_{corr}[a]	G (298 K)
[2233]/[2233]	0	0	0
[2323]/[2323]	0.53	0.70	0.69
M06/6-31+G**//M06/6-31G*:		Relative energies (kcal mol^{-1})	
Conformer	E	E_{corr}[a]	G (298 K)
[2233]/[2233]	0	—	—
[2323]/[2323]	0.67	—	—
Cu-CB-TE2A			
B3LYP/6-31G*//B3LYP/6-31G*:		Relative energies (kcal mol^{-1})	
Conformer	E	E_{corr}[a]	G (298 K)
[2233]/[2233]	1.36	1.55	1.68
[2323]/[2323]	0	0	0
M06/6-31G*//M06/6-31G*:		Relative energies (kcal mol^{-1})	
Conformer	E	E_{corr}[a]	G (298 K)
[2233]/[2233]	1.16	0.58	0.60
[2323]/[2323]	0	0	0
M06/6-31+G**//M06/6-31G*:		Relative energies (kcal mol^{-1})	
Conformer	E	E_{corr}[a]	G (298 K)
[2233]/[2233]	0.68	—	—
[2323]/[2323]	0	—	—

[a] ZPE-corrected

is decreased somewhat for Cu-CB-TE2A but the [2323]/[2323] conformation is still predicted to be favored as observed in the crystal structure.[16] The B3LYP/6-31G*//B3LYP/6-31G* calculations have the two conformations essentially equienergetic for Cu-CB-TE2P and Cu-CB-TE1A1P and favor the [2323]/[2323] conformation strongly for Cu-CB-TE2A, so the trend is similar but shifted toward favoring the [2323]/[2323] conformation. Practical computational limitations prevented us from investigating higher level (triple-zeta) basis sets and our calculations take no account of solvation. Based on benchmarking that has been done in the literature for transition metal complexes and the fact that M06 has been shown to be superior to B3LYP in terms of medium-range correlation energies,[75,77] we are inclined to trust the M06 results more than the B3LYP results. On the basis of the results (Table 2), we tentatively conclude that fundamental differences related to the pendant arm influence the conformation and that the result is not simply a matter of solvation and packing. It is clear from this work that the [2233]/[2233] non-diamond-lattice conformation is energetically viable and must be considered as well as the diamond-lattice [2323]/[2323] conformation as a possible global minimum for cross-bridged metal complexes.

Radiolabeling of CB-TE2P and CB-TE1A1P

Even though cold chemistry experiments showed that the copper(II) complexes of CB-TE1A1P and CB-TE2P formed quickly and under mild conditions in organic solvents (*e.g.*, methanol), radiochemistry experiments were performed in aqueous solvents for translation to *in vivo* investigations. Radiolabeling reactions of ^{64}Cu to CB-TE2P and CB-TE1A1P were performed under aqueous conditions with various buffers, pH values (4.5–8.1), and temperatures (25–95 °C). The radiolabeling yield was determined by radio-HPLC, with the free ^{64}Cu having a retention time of ~4 min and the ^{64}Cu complexes having a retention time of ~20 min. The HPLC peaks corresponding to ^{64}Cu-CB-TE1A1P and ^{64}Cu-CB-TE2P were assigned by LC-MS of a carrier-added sample. Note that under no carrier-added conditions the concentration of the ^{64}Cu complexes was too low to be detected by either UV or MS.

Using mM concentrations of CB-TE2P or CB-TE1A1P, radiolabeling was complete under 1 h, but only at higher temperatures or with carrier-added Cu(II). Using μM concentrations, the CB-TE2P and CB-TE1A1P were labeled with ^{64}Cu at room temperature in shorter time periods. The optimized conditions for ^{64}Cu-labeled CB-TE1A1P and CB-TE2P were as follows: 100 μL of a 26.5 μM solution of chelator in 0.1 M NH_4OAc (pH = 8.1) was incubated with 1 mCi of $^{64}CuCl_2$ at room temperature. Radiochemical yields of >95% were achieved after 30 min. This was the first successful attempt to efficiently radiolabel cross-bridged cyclam derivatives at room temperature. Copper-64-labeling of CB-TE2A under the same conditions resulted in negligible radiochemical yields. As previously reported, CB-TE2A requires temperatures >90 °C in order to achieve complete radiolabeling within 1 h.[18]

Biodistribution studies of ^{64}Cu-CB-TE2P and ^{64}Cu-CB-TE1A1P

In order to gain insight into the pharmacokinetics of the ^{64}Cu-labeled complexes, biodistribution studies were performed. ^{64}Cu-CB-TE2P and ^{64}Cu-CB-TE1A1P (50 μCi (~1 μCi μg^{-1}) in 150 μL of saline) were injected through the tail vein in male, Lewis rats (26 d). The animals were sacrificed at 1, 2, 4 and 24 h after injection, the organs were harvested, and their activity measured with a γ counter. The radiolabeled compounds that were injected for biodistribution studies were positively identified as ^{64}Cu-CB-TE2P and ^{64}Cu-CB-TE1A1P by LC-MS and radio-LC-MS, and were compared to an authentic standard under carrier-added conditions.

As discussed in our communication,[55] ^{64}Cu-CB-TE2P clears rapidly from the blood (from 0.15%ID g^{-1} at 1 h to 0.002%ID/g at 24 h) and has only minor residual uptake in non-target organs such as liver, spleen, lung, heart and marrow (not higher than 0.03%ID g^{-1} at 24 h). Rapid clearance of ^{64}Cu-CB-TE2P from the liver was indicative of its high *in vivo* stability, as it is known that dissociated ^{64}Cu is rapidly coordinated by liver proteins such as superoxide dismutase (SOD), ceruloplasmin and metallothionein and is retained in liver, kidneys and the blood circulation.

A biodistribution study of ^{64}Cu-CB-TE1A1P in Lewis rats (Fig. 5) demonstrated rapid blood clearance (0.08 ± 0.02%ID g^{-1} at 1 h postinjection) and low liver accumulation (0.11 ± 0.01%ID g^{-1} at 1 h postinjection), suggesting that ^{64}Cu-CB-TE1A1P had comparable stability to ^{64}Cu-CB-TE2A and ^{64}Cu-CB-TE2P *in vivo*. Higher uptake was observed in the kidney (1.20 ± 0.43%ID g^{-1} at 1 h postinjection which decreased to 0.30 ± 0.03%ID g^{-1} at 24 h), while no significant uptake was detected in lung, spleen, heart or stomach. These data suggest that ^{64}Cu-CB-TE1A1P clears quickly through the kidneys, with a marginal amount clearing through the liver. Bone uptake cleared significantly by 24 h (0.19 ± 0.04%ID g^{-1} and 0.044 ± 0.003%ID g^{-1} at 1 and 24 h postinjection, respectively). Overall, the biodistribution of CB-TE1A1P was similar to that of CB-TE2P, except for a lower accumulation in the bone at all time points ($p < 0.0001$). Note that unlike the recently-reported 4,11-dimethyl-cyclam-1,8-bis(methylphosphonic acid),[41] both CB-TE2P and CB-TE1A1P form Cu(II) complexes that are suitable for radiopharmaceutical applications because of their inertness *in vivo*, a direct consequence of the cross-bridged bicyclic structure.

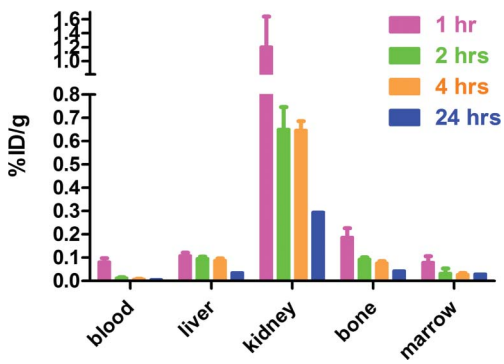

Fig. 5 Biodistribution of ^{64}Cu-CB-TE1A1P (%ID g^{-1}) in male, Lewis rats in selected organs/tissues.

Fig. 6 shows a comparison of the biodistributions of the methanephosphonic acid derivatives of CB-cyclam, ^{64}Cu-labeled CB-TE2P and CB-TE1A1P, compared to CB-TE2A, Diamsar and NOTA. All complexes rapidly clear from the blood, with ^{64}Cu-NOTA showing the highest remaining accumulation at 24 h (0.017 ± 0.001%ID g^{-1}). ^{64}Cu-CB-TE2A has the lowest retention in the marrow, liver and kidney at 24 h postinjection ($p < 0.05$).

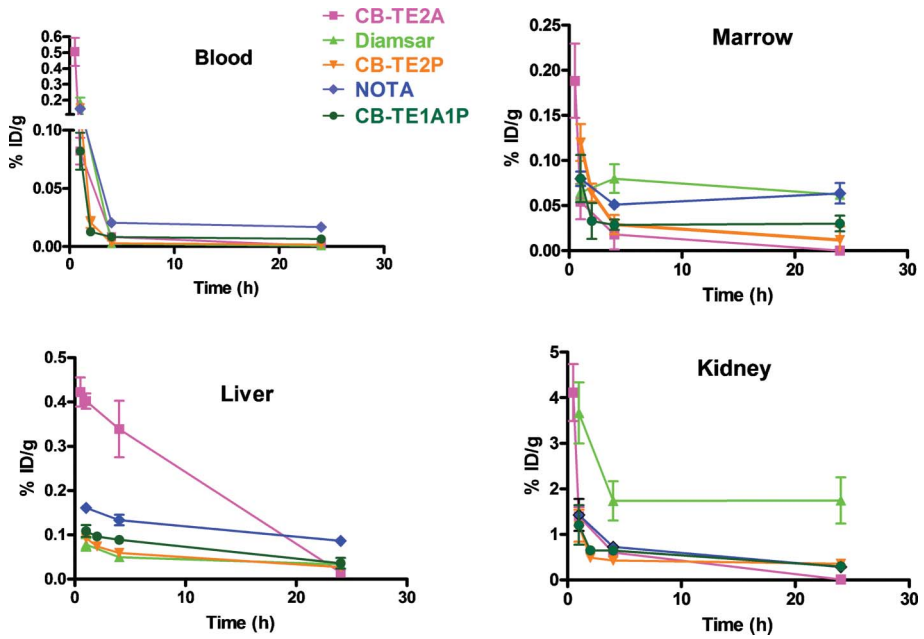

Fig. 6 Comparison of the clearance (%ID g^{-1}) in male Lewis rats of ^{64}Cu-labeled CB-TE2A (□), Diamsar (△), CB-TE2P (▽), NOTA (◇) and CB-TE1A1P (○) from blood, marrow, liver and kidney.

^{64}Cu-NOTA showed significantly higher liver retention (0.086 ± 0.01%ID g^{-1}), while ^{64}Cu-Diamsar has higher kidney retention (1.75 ± 0.50%ID g^{-1}) compared to the other complexes (24 h postinjection; $p < 0.0005$). Overall, ^{64}Cu-CB-TE2P and ^{64}Cu-CB-TE1P demonstrated significantly, but not dramatically, higher accumulations in the marrow, liver and kidneys than ^{64}Cu-CB-TE2A ($p < 0.05$). However, ^{64}Cu-CB-TE2P and ^{64}Cu-CB-TE1P had significantly lower accumulations in the marrow than ^{64}Cu-Diamsar and ^{64}Cu-NOTA, and significantly more clearance from the blood compared to ^{64}Cu-NOTA ($p < 0.05$).

These results are important since CB-TE2P and CB-TE1A1P maintain most of the positive attributes of CB-TE2A including high *in vivo* stability of the ^{64}Cu-complexes; however, a major advantage is that they can be quantitatively labeled at room temperature. ^{64}Cu-CB-TE2A has been shown to have unparalleled *in vivo* stability that is much higher than the commonly used DOTA and TETA chelators. However, the high temperatures required for labeling CB-TE2A with ^{64}Cu have limited its conjugation to only robust peptides and small molecules. CB-TE1A1P will likely eliminate this restriction and allow for its broader use in ^{64}Cu labeling of all types of targeting molecules, including temperature-sensitive proteins such as monoclonal antibodies.

Along with *in vivo* stability, charge and lipophilicity likely play a role in the difference in liver and kidney uptake. For example, the neutral ^{64}Cu-CB-TE2A complex has the highest liver uptake at 1 h post-injection, but has the most extensive clearance of the five complexes, likely due to its superior *in vivo* stability. ^{64}Cu-diamsar, which has a 2+ charge, has the highest retention in the kidneys, and this is consistent with positively charged metal complexes being retained in the kidneys.[78] The macrocycles with the phosphonate pendant arms as well as the NOTA complex of ^{64}Cu(II) are all negatively charged, and thus clear rapidly from the liver and kidneys. To our knowledge, charge does not have a significant impact on blood clearance or retention in the bone marrow.

It is important to emphasize that these data with the ^{64}Cu-chelates may not predict with certainty the *in vivo* stability with ^{64}Cu-labeled chelator-biomolecule conjugates, as the linkage between the chelator and the biomolecule, as well as the nature of the biomolecule have a significant impact on biodistribution. Conjugation of CB-TE1A1P to a biomolecule will result in the conversion of the carboxylate group to an amide moiety. We previously demonstrated that the amide oxygen decreases *in vivo* stability compared to the carboxylate group, and this may negatively impact stability of a CB-TE1A1P-biomolecule conjugate. However, preliminary data from the Anderson lab[79] has demonstrated that a ^{64}Cu-labeled CB-TE1A1P conjugate of the somatostatin analog, Y3-TATE, has a similar biodistribution to ^{64}Cu-CB-TE2A-Y3-TATE,[17] including blood and liver clearance. Maecke *et al.* compared ^{64}Cu-labeled NOTA and CB-TE2A analogs of a somatostatin antagonist, LM3, and a $\alpha_v\beta_3$ integrin-targeted RGD peptide in tumor-bearing mouse models.[80,81] Interestingly, the ^{64}Cu-labeled NOTA (NODAGA) LM3 conjugate showed significantly higher tumor : non-target tissue ratios compared to ^{64}Cu-CB-TE2A-LM3;[80] however, for RGD, the CB-TE2A conjugates showed higher tumor : blood and tumor : liver ratios at 18 h postinjection.[81] This underscores the likelihood that there is not one single Cu(II) chelator that is optimal for all biomolecules.

Summary and conclusions

A new class of cross-bridged cyclam macrocycles having methanephosphonic acid pendant arms has been developed. These compounds readily formed copper(II) complexes and the ^{64}Cu-labeled chelates demonstrate promising kinetic inertness *in vivo*. Both the crystal structures of Cu(II)-CB-TE2P and Cu(II)-CB-TE1A1P showed the copper(II) ion within the bicyclic tetraamine cleft, with the pendant arms completing the coordination sphere

for complete encapsulation of copper. Both crystal structures exhibit the [2233]/[2233] ligand conformation rather than the more common distorted diamond-lattice [2323]/[2323] cross-bridged cyclam conformation found in Cu-CB-TE2A. DFT calculations reproduce this conformational change, which may be a consequence of the longer C–P and P–O bonds in the phosphonate arms as compared to the C–C and C–O bonds of the acetate arms. Acid inertness and electrochemical assays support the viability of these cross-bridged complexes *in vitro*. Biodistribution of ^{64}Cu-CB-TE2P and CB-TE1A1P in normal rats show comparable *in vivo* stability to the current "gold standard", ^{64}Cu-CB-TE2A, but they both have the major advantage of being amenable to ^{64}Cu labeling at room temperature with high specific activity. CB-TE2P and CB-TE1A1P are the first examples of cross-bridged cyclam derivatives that can be radiolabeled with ^{64}Cu at room temperature under no-carrier-added conditions. CB-TE1A1P has the potential for enabling the design of a new generation of imaging agents that can be quickly labeled at room temperature and with high stability *in vivo*, expanding the portfolio of potential agents beyond heat-stable small molecules and peptides into heat-sensitive proteins such as monoclonal antibodies. Bioconjugation of CB-TE1A1P and associated radiolabeling and biological studies toward cancer diagnosis will be reported in future publications.

Experimental

Materials and methods

Reagents: Cupric chloride dihydrate was obtained from Aldrich Chemical Company. Paraformaldehyde and triethyl phosphite were obtained from Acros Organics. 1,1,1,3,3,3-hexafluoro-2-propanol was purchased from Alfa Aesar. Trace Metal™ Grade Hydrochloric acid was obtained from Fischer Scientific. Amberlite CG50 was obtained from Sigma. *Solvents*: Methanol (MeOH, ACS grade) was obtained from Pharmco Products Inc. Diethyl ether (Et_2O) and toluene ($PhCH_3$, ACS grade) were obtained from EMD Chemicals Inc. The solvents were stored in an Innovative Technology Inc. Pure-Solv Solvent Purification System. Prior to use, each solvent was passed through the system's alumina column under low pressure to remove trace impurities.

Melting points (mp) were obtained on a Thomas Hoover capillary melting point apparatus and were uncorrected. Elemental analyses were obtained at Atlantic Microlab Inc., Norcross, GA and Schwartzkopf Microanalytical Laboratory, Woodside, NY. Infrared (IR) spectra were run on a Nicolet MX-1 FT-IR spectrometer and absorptions are reported in wavenumbers (cm^{-1}). High-resolution mass spectra were obtained at the Mass Spectrometry Facility at the University of Notre Dame on a JEOL AX505HA high-resolution mass spectrometer. ^{1}H NMR, ^{13}C{^{1}H} NMR and ^{31}P{^{1}H} NMR spectra were acquired on Varian Mercury-400BB and/or INOVA-500 NMR spectrometers. ^{1}H and ^{13}C chemical shifts are reported in parts per million (ppm) relative to internal Me_4Si (TMS) unless otherwise noted and coupling constants (J) are reported in Hertz (Hz). ^{31}P chemical shifts are reported in parts per million (ppm) relative to an external 85% phosphoric acid standard.

UV-Vis spectra were obtained on a Varian Cary 50 spectrophotometer. Electrochemical studies were performed on a BAS 100B electrochemical analyzer in 0.1 M aq. NaOAc solution using a glassy carbon working electrode, a platinum wire auxiliary electrode, and Ag/AgCl reference electrode. Acid inertness studies were carried out under *pseudo* first-order conditions in 5 M HCl solutions at 90 °C by monitoring the time-dependent decay of the electronic absorption maximum at 630 nm.

Ligand synthesis

CB-TE2A was synthesized as previously published.[16,17] Diamsar[82–84] and NOTA[85] were synthesized as described in the literature.

1,4,8,11-tetraazabicyclo[6.6.2]hexadecane-4,11-bis(methanephosphonic acid diethyl ester) (4). Triethyl phosphite (0.18 mL, 1.0 mmol) and paraformaldehyde (32.5 mg, 2.5 molar equivalents of CH_2O) were added to a solution of 1,4,8,11-tetraazabicyclo[6.6.2]-hexadecane (**3**) (0.0982 g, 0.4338 mmol) in 1.5 mL of dry THF and stirred under N_2 for 4 days. The solvent was removed, the residue was dissolved in H_2O (20 mL), and the solution was made strongly basic (pH = 14, slow addition of KOH pellets). The resulting solution was extracted with toluene (5 × 11 mL), the combined organic phases were dried over anhyd. Na_2SO_4, the solvent was removed under aspirator pressure, and the residual solvent was removed under vacuum to give NMR-pure product (0.2156 g, 94%) as a waxy white solid **4**: mp 42–44 °C; $\nu_{max}(CH_2Cl_2)/cm^{-1}$ 3476, 2980, 2905, 2799, 1669, 1446, 1390, 1366, 1343, 1323, 1292, 1245, 1161, 1126, 1098, 1028; δ_H ($CDCl_3$; 500 MHz; Me_4Si) 1.22–1.32 (14 H, m), 1.32–1.41 (2 H, m), 2.20–2.28 (4 H, m), 2.27–2.35 (2 H, XX′ of AA′XX′, cross-bridge NCH*H*CH*H*N), 2.38 (2 H, dt, J 12.0, 3.2), 2.50–2.75 (6 H, m), 2.60 (2 H, dd, $^2J_{HH}$ −15.6, $^2J_{HP}$ −2.2, NC*H*HP) 2.77–2.87 (2 H, m), 2.82 (2 H, dd (t_{app}), $^2J_{HH}$ −16.0, $^2J_{HP}$ −16.0, NCH*H*P), 3.04–3.13 (2 H, AA′ of AA′XX′, cross-bridge NCH*H*CH*H*N), 3.70 (2 H, tt, J 11.7, 4.2), 3.99–4.10 (8 H, m, P(O)OC*H*$_2$CH$_3$); δ_C ($CDCl_3$, 125.68 MHz, Me_4Si) 15.54 (2 C, d, $^3J_{PC}$ 4.8, OCH$_2$*C*H$_3$), 15.59 (2 C, d, $^3J_{PC}$ 5.8, OCH$_2$*C*H$_3$), 27.10 (C-6, 13), 49.24 (2 C, d, $^1J_{PC}$ 160.3, N*C*H$_2$P), 49.88 (coincident with downfield line of d at 49.24), 54.94 (2 C, d $^3J_{PC}$ 15.4, C-5, 12), 55.55, 55.79 (C-15, 16), 59.41, 60.24 (2 C, d, $^2J_{PC}$ 6.7, O*C*H$_2$CH$_3$), 60.47 (2 C, d, $^2J_{PC}$ 7.7, O*C*H$_2$CH$_3$); [Note: ^{1}H-COSY and gHMQC experiments aided resonance assignments (see structure below for compound numbering)]; δ_P ^{31}P{^{1}H} ($CDCl_3$, 161.83 MHz, external 85% phosphoric acid) 26.98; HRFABMS, m/z $(M+H)^+$ exact mass for $C_{22}H_{49}N_4O_6P_2$: 527.3127; Found: 527.3119 (error −0.8 mmu/−1.6 ppm).

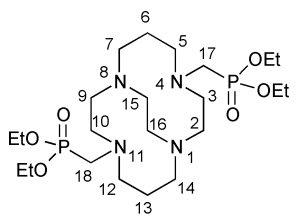

Numbering for **4**

1,4,8,11-Tetraazabicyclo[6.6.2]hexadecane-4,11-bis(methanephosphonic acid) (1·0.6 HCl·1.1H$_2$O). Bis(phosphonate ester) **4** (0.3440 g, 0.6533 mmol) was dissolved in 6 M HCl (32 mL) and refluxed under N_2 for 1 day. The solvent was removed under reduced pressure and the crude product was dissolved in

H_2O (4 mL) and chromatographed using a weakly acidic cation exchange column (Amberlite CG50, H^+ form, 7.7 g, column size = 27 cm × 2 cm). The product was eluted with H_2O (first 30 mL of eluant was discarded), fractions containing the product were combined (35 fractions, 3 mL each), the solvent was removed under reduced pressure, and residual solvent was removed under vacuum to give **2**·0.6HCl·1.1H_2O (0.1919 g, 64%) as a white solid: mp 182–185 °C (Found: C, 36.56; H, 7.84; N, 12.06; Cl, 4.81. Calc. for $C_{14}H_{32}N_4O_6P_2\cdot(HCl)_{0.6}\cdot(H_2O)_{1.1}$: C, 36.87; H, 7.69; N 12.28; Cl, 4.66%); ν_{max}(KBr)/cm^{-1} 3397 (br), 2983, 2851, 1655, 1491, 1470, 1241, 1183, 1097, 1073, 1047, 903; δ_H (D_2O; 500 MHz; internal ref CH_3CN set to 2.06) 1.74–1.83 (2 H, dm, *J* 16.6, 6-H$_{eq}$), 2.29–2.42 (2 H, qm-like, 6-H$_{ax}$), 2.49–2.58 (2 H, dm, *J* 13.9, 2-H$_{eq}$), 2.80–2.93 (4 H, m, 15-H BB′ of AA′BB′ and 7-H), 2.95–3.18 (8 H, m, 15-H AA′ of AA′BB′, 7-H, 3-H$_{eq}$, NC*H*HP), 3.29–3.37 (2 H, dm, *J* 13.2, 5-H$_{eq}$), 3.45 (2 H, td, *J* 13.7, 3.7, 2-H$_{ax}$), 3.76 (2 H, tt$_{app}$, *J* 14.6, 3.7, 3-H$_{ax}$), 3.96 (2 H, td, *J* 13.0, 3.4, 5-H$_{ax}$), and 4.17 (2 H, dd (t$_{app}$), $^2J_{HH}$ −14.6, $^2J_{PC}$ −14.6, NCH*H*P); δ_C (D_2O, 125.68 MHz, internal *C*H_3CN set to 1.47) 20.23 (C-6), 48.75 (C-15), 52.01 (2 C, d, $^1J_{PC}$ 137.2, N*C*H_2P), 52.34 (2 C, d, $^3J_{PC}$ 9.6, C-3), 52.64 (C-2), 58.17 (br, C-5), 58.47 (C-7) [Note: ^{1}H-COSY and gHMQC experiments aided resonance assignments (see structure below for compound numbering)]; δ_P ^{31}P{^{1}H} (D_2O, 161.83 MHz, external 85% phosphoric acid) 9.48 (s); HRFABMS, *m*/*z* (M+H)$^+$ exact mass for $C_{14}H_{33}N_4O_6P_2$: 415.1875; Found: 415.1877 (error +0.1 mmu/+0.4 ppm). Diffusion of acetone into an aqueous solution of **1**·0.6HCl·1.1H_2O produced crystals suitable for X-ray diffraction.

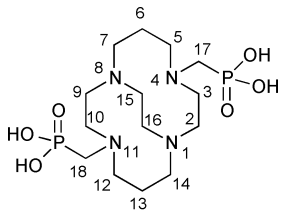

Numbering for **1**

1,4,8,11-tetraazabicyclo[6.6.2]hexadecane-4-(methanephosphonic acid diethyl ester)-11-(methanecarboxylic acid *tert*-butyl ester) (6). Triethyl phosphite (27 µL, 0.16 mmol) and paraformaldehyde (4.9 mg, 0.16 mmol) were added to a solution of 1,4,8,11-tetraazabicyclo[6.6.2]hexadecane-4-(methanecarboxylic acid *tert*-butyl ester)[19] (**5**, 30 mg, 0.088 mmol) in dry THF (2 mL) and stirred under N_2 for 4 days. The solvent was removed, the residue was dissolved in H_2O (10 mL), and the solution was made strongly basic (pH = 14, slow addition of KOH pellets). The resulting solution was extracted with toluene (3 × 10 mL) and CH_2Cl_2 (3 × 10 mL), the combined organic phases were dried over anhyd. Na_2SO_4, the solvent was removed under reduced pressure, and the residual solvent was removed under vacuum to give reasonably pure product by NMR (35 mg, 81%) as an oil. δ_H (500 MHz; C_6D_6; Me_4Si) 1.07 (3 H, t, *J* 7.1, P(O)CH$_2$C*H*$_3$), 1.10 (3 H, t, *J* 7.1, P(O)CH$_2$C*H*$_3$), 1.20–1.43 (4 H, m, 6-H, 13-H), 1.36 (4 H, br s, 2*H*$_2$O), 1.40 (9 H, s, C(C*H*$_3$)), 2.22–2.31 (3 H, m), 2.35–2.41 (2 H, m), 2.48–2.99 (10 H, m), 2.57 (1 H, overlapped m, 18-H; located by gHMQC and ^{1}H/^{31}P gHMQC), 2.86 (1 H, dd, $^2J_{HH}$ and $^2J_{PH}$ −17.6, −15.6, H-18′; located by gHMQC and ^{1}H/^{31}P gHMQC), 3.03 (1 H, B of AB, *J* −16.4, 17-H), 3.10 (1 H, ddd, *J* 13.7, 11.5, 3.9), 3.18 (1 H, A of AB, *J* −16.4, 17-H′), 3.305–3.415 (2 H, sym m), 3.63 (1 H, td, *J* 12.0, 4.1), 3.85–3.96 (1H, m), 3.88–4.08 (4 H, m, 2 P(O)C*H*$_2$CH$_3$); δ_C ^{13}C{^{1}H} (125.68 MHz; C_6D_6; central solvent peak set to δ 128.06) 16.71 (d, $^3J_{PC}$ 5.7, P(O)*C*H$_2$CH$_3$), 16.77 (d, $^3J_{PC}$ 5.7, P(O)*C*H$_2$CH$_3$), 28.29 (C(*C*H$_3$)$_3$), 28.34, 28.79, 51.06 (d, $^1J_{PC}$ 163.9, C-18), 51.21 (2 C), 53.60, 56.01 (C-18), 56.40 (d, $^3J_{PC}$ 16.4), 56.69, 56.90, 57.38, 57.54, 60.46, 60.88, 61.05 (d, $^2J_{PC}$ 6.7, P(O)*C*H$_2$CH$_3$), 61.37 (d, $^2J_{PC}$ 6.7, P(O)*C*H$_2$CH$_3$), 79.90 (*C*(CH$_3$)$_3$), 171.27 (*C*OOH) [Notes: ^{1}H-COSY, gHMQC and ^{1}H/^{31}P gHMQC experiments aided resonance assignments; ^{31}P-^{13}C couplings were confirmed by obtaining ^{13}C{^{1}H} spectra at two different frequencies, 125 MHz and 100 MHz]; δ_P ^{31}P{^{1}H} (202.31 MHz; C_6D_6; external reference 85% phosphoric acid set to δ 0.00) 26.46 (s).

The reaction was also scaled up and the product carried directly to the next step: Triethyl phosphite (0.18 mL, 1.0 mmol) and paraformaldehyde (32.5 mg, 2.5 molar equivalents of CH_2O) were added to a solution of **5** (200 mg, 0.587 mmol) in dry THF (4 mL) and stirred under N_2 for 4 days. Solvent was removed, the residue was dissolved in H_2O (20 mL), and the solution was made strongly basic (pH = 14, slow addition of KOH pellets). The resulting solution was extracted with toluene (5 × 20 mL), the combined organic phases were dried over anhyd. Na_2SO_4, and solvent was removed to give crude product (0.29 g, oil) that was used for the next reaction without further purification.

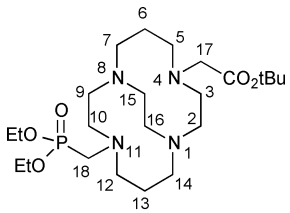

Numbering for **6**

1,4,8,11-Tetraazabicyclo[6.6.2]hexadecane-4-(methanephosphonic acid)-11-methanecarboxylic acid (2·0.45HCl·2H_2O). Crude **6** (0.29 g) from the previous step was dissolved in 35 mL of 6 M HCl and refluxed under N_2 for 1 day. The solvent was removed under reduced pressure and the crude product was dissolved in 4 mL of H_2O and chromatographed using a weakly acidic cation exchange column (Amberlite CG50, H^+ form, 7.7 g, column size = 27 cm × 2 cm). The product was eluted with H_2O (first 30 mL of eluant was discarded), fractions containing the product were combined (35 fractions, 3 mL each), the solvent was removed under reduced pressure, and residual solvent was removed under vacuum to give the desired product as a white solid hydrated hydrochloride (0.157 g, 0.365 mmol, 62% yield from **5**): mp >250 °C. Elemental analysis: found: C, 41.97; H, 8.13; N, 12.65; Cl, 3.93. Calc. for $C_{15}H_{31}N_4O_5P\cdot0.45(HCl)\cdot2(H_2O)$: C, 41.82; H, 8.29; N 13.00; Cl, 3.70%; HR-ESI-MS, *m*/*z* (M–H) exact mass for $C_{15}H_{30}N_4O_5P$: 377.1959; Found: 377.1953 (error +1.6 ppm). It has also been shown that the product can be further purified if necessary by reversed-phase HPLC on a C18 semi-preparative column (gradient 0.1% TFA in H_2O/0.1% TFA in MeCN; details may be found in the ESI†). LC-MS results confirmed purity (see ESI for details†). Product purified in this manner (TFA salt) gave the following spectroscopic and analysis data: δ_H (500 MHz; D_2O; internal reference CH_3CN set to δ 2.06) 1.73–1.80 (1 H, dm, *J* 16.6, 6-H$_{eq}$),

1.79–1.86 (1 H, dm, J 16.9, 13-H$_{eq}$), 2.33–2.45 (2 H, m, 6-H$_{ax}$, 13-H$_{ax}$), 2.57 (1 H, ddd, J 13.7, 3.6, 1.3, 2-H$_{eq}$), 2.85 (1 H, dt, J 14.2, 2.4, 9-H$_{eq}$), 2.88–3.35 (13 H, m), 3.08 (1 H, dd, $^{2}J_{HH}$ 14.7, $^{2}J_{PH}$ 10.6, 18-H), 3.55 (1 H, ddd, J 14.8, 13.4, 3.6, 3-H$_{ax}$), 3.61 (1 H, d, J 17.0, 17-H), 3.65 (1 H, dd (t$_{app}$), $^{2}J_{HH}$ 14.8, $^{2}J_{PH}$ 14.8, 18-H′), 3.70 (1 H, td, J 13.8, 3.1, 9-H$_{ax}$), 3.82–3.90 (1 H, m, 10-H$_{ax}$), 4.04 (1 H, td, J 13.1, 3.7, 12-H$_{ax}$), 4.34 (1 H, d, J 17.0, 17-H′); δ_C (125.68 MHz; D_2O; internal reference CH_3CN set to δ 1.47) 19.71 (C-6), 20.17 (C-13), 47.78, 48.55, 49.13 (C-3), 51.35 (d, $^{1}J_{PC}$ 139.1, C-18), 51.71 (d, $^{3}J_{PC}$ 10.5, C-10), 52.83 (C-9), 53.83 (C-2), 55.75 (C-17), 58.21 (C-12), 58.36 (C-5), 58.81, 59.39, 116.88 (q, $^{1}J_{CF}$ 291.4, CF_3COOH), 163.44 (q, $^{2}J_{CF}$ 35.8, CF_3COOH), 172.44 ($COOH$) [Notes: ^{1}H-COSY, gHMQC, and gHMBC experiments aided resonance assignments; ^{31}P-^{13}C couplings were confirmed by obtaining ^{13}C{^{1}H} spectra at two different frequencies, 125 MHz and 100 MHz]; δ_P ^{31}P{^{1}H} (202.31 MHz; D_2O; external reference 85% phosphoric acid set to δ 0.00) 9.24 (s); Found: C, 35.56; H, 5.3; N, 8.4; F, 20.9. Calc. for $C_{15}H_{31}N_4O_5P{\cdot}2.5(CF_3COOH){\cdot}H_2O$: C, 35.25; H, 5.25; N, 8.2; F, 20.9%.

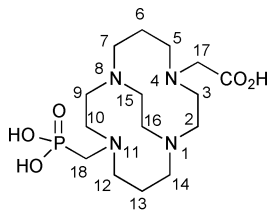

Numbering for **2**

Copper(II) complex synthesis

Cu-CB-TE2P. A solution of $CuCl_2{\cdot}2H_2O$ (0.0132 g, 0.077 mmol) in 2 mL MeOH was added to a 2 mL solution of **1**·0.6HCl·1.1H_2O (0.035 g, 0.077 mmol) in MeOH. Aq. NaOH (0.3 mL of a 0.4 M solution) was added to raise the pH to 5. The resulting blue solution was evaporated to dryness and extracted with 1 mL of 1,1,1,3,3,3-hexafluoro-2-propanol. The NaCl precipitate was separated from the blue supernatant after centrifugation. Diethyl ether diffusion into the supernatant yielded blue microcrystals (0.047 g, 86%) (Found: C, 29.48; H, 4.96; N, 7.91; Cl, 1.78; P, 8.66. Calc. for $C_{14}H_{30}N_4O_6P_2Cu{\cdot}H_2O{\cdot}0.3NaCl{\cdot}1.2C_3H_2F_6O$: C, 29.64; H, 4.86; N, 7.86; Cl, 1.49; P 8.69%); UV-Vis: λ_{max} (MeOH)/nm 639 (ε/dm^3 mol^{-1} cm^{-1} 35); HRFABMS m/z (M+H)$^+$ exact mass for $C_{14}H_{31}N_4P_2Cu$: 476.1015; Found: 476.1009 (error –0.6 mmu/–1.2 ppm). Cyclic voltammogram (0.1 M aq. NaOAc): –0.96 V (Ag/AgCl) *quasi*-reversible. X-ray crystals were obtained by diethyl ether diffusion into a hexafluoro-2-propanol solution of the complex inside a 2 mm inner diameter glass tube.

Cu-CB-TE1A1P. An amount of CB-TE1A1P·0.45HCl·2H_2O (84 mg, 0.19 mmol) was dissolved in 2 mL water along with $Cu(ClO_4)_2{\cdot}6H_2O$ (75 mg, 0.20 mmol). The solution pH was adjusted to 2 using 0.1 N NaOH and stirred for 1 h. After removal of solvent by rotary evaporation, the blue residue was dissolved in 1 mL of methanol. After a small amount of insoluble material was removed by centrifugation, the supernatant was placed in a vial inside a chamber and diethyl ether allowed to diffuse into it. After 2 days, a dark-blue solid deposited which was separated and dried. About 1 mL of hexafluoro-isopropanol was added to this solid and the resulting suspension centrifuged to remove a small amount of insoluble matter. The supernatant was returned to the ether diffusion chamber yielding a dark-blue solid product (120 mg, 95% yield) upon standing. Elemental analysis: found: C, 31.71; H, 4.72; N, 8.04; Cl, 3.12. Calc. for $CuC_{15}H_{29}N_4O_5P{\cdot}C_3F_6OH_2{\cdot}0.60(NaClO_4)$: C, 31.73; H, 4.58; N, 8.22; Cl, 3.12%. UV-Vis: λ_{max} (aq)/nm 613 (ε/dm^3 mol^{-1} cm^{-1} 24); FT-IR (KBr): 1619, 1262, 1218, 1100 cm^{-1}. Cyclic voltammetry (0.1 M NaOAc, 40 mV s^{-1}): reduction peak potential –1.03 V (irrev, Ag/AgCl), copper stripping peak +0.10 V. Crystals suitable for X-ray diffraction study were obtained by slow evaporation of a 6 M aqueous ammonia sample solution.

X-ray structural studies

A summary of crystal data for the two X-ray structures can be found in Table 3.

Cu-CB-TE2P. A crystal was mounted on a Cryoloop with Paratone-N oil and cooled to –173 °C under a stream of dry nitrogen gas. Data were collected on a BRUKER APEX2 CCD X-ray system using Cu K alpha radiation at –173 °C and integrated using APEX2 software (SHELXL) corrected for adsorption using SADABS. Structure was solved by direct methods and all non-hydrogen atoms were refined as being anisotropic. Two molecules were found in the asymmetric unit. One of the molecules was disordered and this was treated by assuming a two-position disorder model. Although all the hydrogen atoms were not found, they were included in the chemical formula to account for F000, density and molecular weight.

Disorder associated with Cu-CB-TE2P was treated by using a 50% occupancy model for atoms C15, C16, C17, C18, C23, C24, C25, C26, C27, N5, N6, O7, O8, O9, P3, O2SA, O2SB, O6SA, O6SB, C15′, C16′ C17′, C18′, C23′, C24′, C25′, C26′ C27′, N5′, N6′, O7′, O8′, O9′, P3′ and their associated hydrogen atoms. Occupancies were set for the following atoms at values indicated: Atoms O5SA 40%, O5SB 60%, O7SA and O7SB both at 30% occupancy while O7SC was at 40% occupancy; atoms Na1A and Na1B 75% and 25%, respectively. The hydrogen atoms on O8 and O8′ were fixed in position with appropriate riding models.

Cu-CB-TE1A1P. A blue crystal was mounted on a Cryoloop with Paratone-N oil. Data were collected on a Bruker APEX II CCD system using Mo K alpha radiation in a nitrogen gas stream at 100(2) K using phi and omega scans. Crystal-to-detector distance was 60 mm and exposure time was 10 s per frame using a scan width of 0.5°. Indexing and unit cell refinement indicated a primitive, orthorhombic lattice. The space group was found to be *Pccn*. The data were integrated using the Bruker SHELXTL software program and scaled using the SADABS software program. Solution by direct methods (SHELXS) and all non-hydrogen atoms were refined anisotropically by full-matrix least-squares (SHELXL-97). All hydrogen atoms except H2P on O2 were placed on their appropriate parent atom using a riding model. Hydrogen H2P was determined from a Fourier difference map and was allowed to refine. Hydrogen atoms on water molecules were restrained using DFIX and DANG commands.

Radiochemistry

$^{64}Cu(OAc)_2$ was obtained by adding 200 μL of 0.4 M NH_4OAc (pH = 6.5) to 5 mCi of $^{64}CuCl_2$ in 5 μL of 2 M HCl and shaking the reaction for 10 min at room temperature.

Table 3 Crystal data and structure refinement for Cu-CB-TE2P and Cu-CB-TE1A1P

Cu-CB-TE2P		
Empirical formula	$C_{14}H_{34}Cl_{0.50}CuN_4Na_{0.50}O_{9.50}P_2$	
Formula weight	565.15	
Temperature	100(2) K	
Wavelength	1.54178 Å	
Crystal system	Triclinic	
Space group	$P\bar{1}$	
Unit cell dimensions	a = 9.5428(5) Å	α = 80.039(4)°
	b = 15.5173(7) Å	β = 81.081(4)°
	c = 16.9240(10) Å	γ = 89.874(3)°
Volume	2437.7(2) Å3	
Z	4	
Density (calculated)	1.540 g cm^{-3}	
Absorption coefficient	3.574 mm^{-1}	
F(000)	1180	
Crystal size	0.31 × 0.21 × 0.05 mm^3	
Theta range for data collection	4.28 to 59.37°	
Index ranges	−10 ≤ h ≤ 10, −17 ≤ k ≤ 17, −16 ≤ l ≤ 18	
Reflections collected	16637	
Independent reflections	6611 [R(int) = 0.0970]	
Completeness to theta = 59.37°	92.9%	
Absorption correction	None	
Refinement method	Full-matrix least-squares on F2	
Data/restraints/parameters	6611/0/593	
Goodness-of-fit on F2	1.020	
Final R indices [$I > 2\sigma(I)$]	R_1 = 0.0741, wR_2 = 0.1968	
R indices (all data)	R_1 = 0.1213, wR_2 = 0.2186	
Largest diff. peak and hole	0.941 and −0.730 e Å^{-3}	

Cu-CB-TE1A1P		
Empirical formula	$C_{30}H_{80}Cu_2N_8O_{21}P_2$	
Formula weight	1078.04	
Temperature	100(2) K	
Wavelength	0.71073 Å	
Crystal system	Orthorhombic	
Space group	Pccn	
Unit cell dimensions	a = 10.1989(19) Å	α = 90°.
	b = 35.067(7) Å	β = 90°.
	c = 12.943(3) Å	γ = 90°.
Volume	4629.2(15) Å3	
Z	4	
Density (calculated)	1.547 Mg m^{-3}	
Absorption coefficient	1.073 mm^{-1}	
F(000)	2288	
Crystal size	0.20 × 0.20 × 0.10 mm^3	
Crystal color/habit	blue/plate	
Theta range for data collection	2.08 to 28.29°.	
Index ranges	−13 ≤ h < = 13, −46 ≤ k ≤ 45, −16 ≤ l ≤ 17	
Reflections collected	57822	
Independent reflections	5510 [R(int) = 0.0564]	
Completeness to theta = 25.00°	99.9%	
Absorption correction	multi-scan/sadabs	
Max. and min. transmission	0.9003 and 0.8141	
Refinement method	Full-matrix least-squares on F2	
Data/restraints/parameters	5510/17/322	
Goodness-of-fit on F2	1.157	
Final R indices [$I > 2\sigma(I)$]	R_1 = 0.0484, wR_2 = 0.1350	
R indices (all data)	R_1 = 0.0568, wR_2 = 0.1392	
Largest diff. peak and hole	0.585 and −0.520 e.Å^{-3}	

Preparation of ^{64}Cu-CB-TE2P and ^{64}Cu-CB-TE1A1P. A 25 μM stock solution was obtained by dissolving the chelator in 0.1 M NH_4OAc, pH = 8.1. $^{64}CuCl_2$ was added to 100 μL of the stock solution (1 mCi of ^{64}Cu per 1 μg of CB-TE2P or CB-TE1A1P) and the resulting solution was shaken for 30 min at room temperature. The outcome of the labeling experiment was determined by radio-HPLC (C_8 analytical column, isocratic 0.1% TFA in water, 0.5 mL min^{-1}). Free ^{64}Cu has a retention time of approximately 4 min while the radiolabeled compound has a retention time of approximately 20 min.

Preparation of ^{64}Cu-CB-TE2P for rat biodistribution. CB-TE2P (0.83 mg) was dissolved in 1 mL of 0.4 M NH_4OAc (pH = 6.5) and 1.0 mCi of $^{64}Cu(OAc)_2$ (50 μL) in 0.4 M NH_4OAc (pH = 6.5) was added with shaking at 95 °C for 1 h resulting in 100% radiochemical purity by radio-TLC (C18 plates, eluant : methanol/10% ammonium acetate 1 : 4). The ^{64}Cu-CB-TE2P was diluted with 2.7 mL of saline and divided into 150 μL aliquots (42 μg chelator; 45 μCi ^{64}Cu per dose).

Preparation of ^{64}Cu-CB-TE1A1P for rat biodistribution. CB-TE1A1P (1.2 mg) was dissolved in 200 μL of 0.1 M NH_4OAc (pH = 7) and 1.1 mCi of $^{64}Cu(OAc)_2$ (400 μL) in 0.4 M NH_4OAc (pH = 6.5) were incubated with shaking at 95 °C for 1 h resulting in 100% radiochemical purity by radio-TLC (C18 plates, eluant: methanol/10% ammonium acetate 1 : 4). The ^{64}Cu-CB-TE1A1P was diluted with 3.15 mL of saline and divided into 150 μL aliquots (48 μg chelator; 40 μCi each).

Preparation of ^{64}Cu-CB-TE2A, ^{64}Cu-NOTA and ^{64}Cu-Diamsar. ^{64}Cu-CB-TE2A was prepared as previously described.[86] ^{64}Cu-NOTA was prepared by incubating a solution of $^{64}CuCl_2$ (1.3 mCi, 50 μL, 0.1 M NH_4OAc, pH 7.0) with 4.17 μg of NOTA dissolved in 50 μL of 0.1 M NH_4OAc, pH 7.0. The reaction mixture was heated to 37 °C for 1 h and radiochemical purity of ≥98% was attained as followed by radio-TLC.

^{64}Cu-Diamsar was prepared by incubating the chelator (1 mg) with ^{64}Cu in 0.5 M NH_4OAc buffer (pH = 10) at room temperature in 30 min. A single peak (R_f ~ 0.2) corresponding to ^{64}Cu-Diamsar was verified by radio-TLC using a mobile phase of ethanol on ITLC-SG plates (R_f (^{64}Cu-acetate) = 0). Radiochemical purity of ^{64}Cu-Diamsar was > 95% as confirmed by radio-TLC and radio-HPLC (retention time (^{64}Cu-Diamsar) = 32 min). HPLC analysis of the radiolabeled complex was performed using an EPS column with the following gradient: solvent A: 10 mM NH_4OAc, pH 5.5; solvent B: 0.1% TFA in acetonitrile; 0% B to 50% B in 40 min; 0.5 mL min^{-1} flow rate.

The Cu(II) complex of Diamsar (^{nat}Cu-Diamsar) was prepared with high-purity natural copper chloride ($CuCl_2$) using the procedure described above except both non-radioactive $CuCl_2$ and radioactive $^{64}CuCl_2$ (~50 μCi) were added to the reaction mixture. Complex formation was determined by radio-TLC and confirmed by radio-HPLC. After sufficient time for radio-decay, formation of ^{nat}Cu-Diamsar was demonstrated by ESI-MS (calc. m/z $(M–H)^+$, 376.23; found, 376.20).

Biodistribution studies

Animal experiments were carried out in compliance with the Guidelines for the Care and Use of Research Animals established by the Animal Studies Committee of Washington University.

Male Lewis rats (34–35 day old) were injected with ^{64}Cu-NOTA, ^{64}Cu-Diamsar, ^{64}Cu-CB-TE2P or ^{64}Cu-CB-TE1A1P (40–60 μCi; 0.5–130 nmol ligand) intravenously *via* the tail vein. Tissue biodistribution data were obtained at 1, 4, and 24 h postinjection. Animals were sacrificed at 1, 4 and 24 h postinjection, organs of interest were removed, weighed, and counted on a gamma counter (Beckman). The percent injected dose per gram (%ID g^{-1}) and percent injected dose per organ (%ID organ^{-1}) were measured by comparison against a weighed, counted standard.

Computational chemistry

All DFT calculations were carried out in parallel mode using Spartan'10 version 1.1.0 (Wavefunction, Inc., Irvine, CA) running the Q-Chem computational engine[87] on a Mac Pro dual Quad-Core Intel Xeon (2.93 GHz) computer with 16 GB of RAM.

Acknowledgements

This work was supported by Award Number R01CA093375 from the National Cancer Institute (USA). The content is solely the responsibility of the authors and does not necessarily represent the official views of the National Cancer Institute or the National Institutes of Health. The authors thank Elizabeth Garcia (University of New Hampshire) for synthesis of NOTA and Christopher D. Sherman (Washington University) for performing the biodistribution studies.

Notes and references

1 S. Bhattacharyya and M. Dixit, *Dalton Trans.*, 2011, **40**, 6112–6128.
2 T. J. Wadas, E. H. Wong, G. R. Weisman and C. J. Anderson, *Chem. Rev.*, 2010, **110**, 2858–2902.
3 C. J. Anderson and M. J. Welch, *Chem. Rev.*, 1999, **99**, 2219–2234.
4 D. W. McCarthy, R. E. Shefer, R. E. Klinkowstein, L. A. Bass, W. H. Margenau, C. S. Cutler, C. J. Anderson and M. J. Welch, *Nucl. Med. Biol.*, 1997, **24**, 35–43.
5 P. S. Donnelly, *Dalton Trans.*, 2011, **40**, 999–1010.
6 B. M. Zeglis and J. S. Lewis, *Dalton Trans.*, 2011, **40**, 6168.
7 R. E. Mewis and S. J. Archibald, *Coord. Chem. Rev.*, 2010, **254**, 1686–1712.
8 M. Shokeen and C. J. Anderson, *Acc. Chem. Res.*, 2009, **42**, 832–841.
9 T. J. Wadas, E. H. Wong, G. R. Weisman and C. J. Anderson, *Curr. Pharm. Des.*, 2007, **13**, 3–16.
10 S. V. Smith, *J. Inorg. Biochem.*, 2004, **98**, 1874–1901.
11 K. S. Woodin, K. J. Heroux, C. A. Boswell, E. H. Wong, G. R. Weisman, W. J. Niu, S. A. Tomellini, C. J. Anderson, L. N. Zakharov and A. L. Rheingold, *Eur. J. Inorg. Chem.*, 2005, 4829–4833.
12 M. K. Moi, C. F. Meares, M. J. Mccall, W. C. Cole and S. J. Denardo, *Anal. Biochem.*, 1985, **148**, 249–253.
13 W. C. Cole, S. J. Denardo, C. F. Meares, M. J. Mccall, G. L. Denardo, A. L. Epstein, H. A. Obrien and M. K. Moi, *J. Nucl. Med.*, 1987, **28**, 83–90.
14 L. A. Bass, M. Wang, M. J. Welch and C. J. Anderson, *Bioconjugate Chem.*, 2000, **11**, 527–532.
15 C. A. Boswell, X. K. Sun, W. J. Niu, G. R. Weisman, E. H. Wong, A. L. Rheingold and C. J. Anderson, *J. Med. Chem.*, 2004, **47**, 1465–1474.
16 E. H. Wong, G. R. Weisman, D. C. Hill, D. P. Reed, M. E. Rogers, J. S. Condon, M. A. Fagan, J. C. Calabrese, K. C. Lam, I. A. Guzei and A. L. Rheingold, *J. Am. Chem. Soc.*, 2000, **122**, 10561–10572.
17 J. E. Sprague, Y. J. Peng, X. K. Sun, G. R. Weisman, E. H. Wong, S. Achilefu and C. J. Anderson, *Clin. Cancer Res.*, 2004, **10**, 8674–8682.
18 X. K. Sun, M. Wuest, G. R. Weisman, E. H. Wong, D. P. Reed, C. A. Boswell, R. Motekaitis, A. E. Martell, M. J. Welch and C. J. Anderson, *J. Med. Chem.*, 2002, **45**, 469–477.
19 J. E. Sprague, Y. Peng, A. L. Fiamengo, K. S. Woodin, E. A. Southwick, G. R. Weisman, E. H. Wong, J. A. Golen, A. L. Rheingold and C. J. Anderson, *J. Med. Chem.*, 2007, **50**, 2527–2535.
20 T. J. Wadas, M. Eiblmaier, A. Zheleznyak, C. D. Sherman, R. Ferdani, K. Liang, S. Achilefu and C. J. Anderson, *J. Nucl. Med.*, 2008, **49**, 1819–1827.
21 T. J. Wadas and C. J. Anderson, *Nat. Protoc.*, 2006, **1**, 3062–3068.
22 J. E. Sprague, H. Kitaura, W. Zou, Y. Ye, S. Achilefu, K. N. Weilbaecher, S. L. Teitelbaum and C. J. Anderson, *J. Nucl. Med.*, 2007, **48**, 311–318.
23 L. Wei, Y. Ye, T. Wadas, J. S. Lewis, M. J. Welch, S. Achilefu and C. J. Anderson, *Nucl. Med. Biol.*, 2009, **36**, 277–285.
24 L. Wei, C. Butcher, Y. Miao, F. Gallazzi, T. P. Quinn, M. J. Welch and J. S. Lewis, *J. Nucl. Med.*, 2007, **48**, 64–72.
25 J. C. Garrison, T. L. Rold, G. L. Sieckman, S. D. Figueroa, W. A. Volkert, S. S. Jurisson and T. J. Hoffman, *J. Nucl. Med.*, 2007, **48**, 1327–1337.
26 W. Liu, G. Hao, M. A. Long, T. Anthony, J.-T. Hsieh and X. Sun, *Angew. Chem., Int. Ed.*, 2009, **48**, 7346–7349.
27 E. Lewis, R. Boyle and S. Archibald, *Chem. Commun.*, 2004, 2212–2213.
28 C. A. Boswell, C. A. S. Regino, K. E. Baidoo, K. J. Wong, A. Bumb, H. Xu, D. E. Milenic, J. A. Kelley, C. C. Lai and M. W. Brechbiel, *Bioconjugate Chem.*, 2008, **19**, 1476–1484.
29 A. Y. Lebedev, J. P. Holland and J. S. Lewis, *Chem. Commun.*, 2010, 1706–1708.
30 I. Svobodová, P. Lubal, J. Plutnar, J. Havlícková, J. Kotek, P. Hermann and I. Lukes, *Dalton Trans.*, 2006, 5184–5197.
31 F. K. Kalman, Z. Baranyai, I. Toth, I. Banyai, R. Kiraly, E. Brucher, S. Aime, X. K. Sun, A. D. Sherry and Z. Kovacs, *Inorg. Chem.*, 2008, **47**, 3851–3862.
32 C. Bianchini, G. Giambastiani, F. Laschi, P. Mariani, A. Vacca, F. Vizza and P. Zanello, *Org. Biomol. Chem.*, 2003, **1**, 879–886.
33 C. F. G. C. Geraldes, M. P. M. Marques, B. de Castro and E. Pereira, *Eur. J. Inorg. Chem.*, 2000, 559–565.
34 J. Kotek, P. Lubal, P. Hermann, I. Cisarova, I. Lukes, T. Godula, I. Svobodova, P. Taborsky and J. Havel, *Chem.–Eur. J.*, 2003, **9**, 233–248.
35 S. Füzerová, J. Kotek, I. Císařová, P. Hermann, K. Binnemans and I. Lukeš, *Dalton Trans.*, 2005, **2005**, 2908–2915.
36 K. P. Guerra, R. Delgado, L. S. M. P. Lima, M. G. B. Drew and V. T. Felix, *Dalton Trans.*, 2004, 1812–1822.
37 P. Lubal, M. Kyvala, P. Hermann, J. Holubova, J. Rohovec, J. Havel and I. Lukes, *Polyhedron*, 2001, **20**, 47–55.
38 J. Kotek, F. K. Kalman, P. Hermann, E. Brucher, K. Binnemans and I. Lukes, *Eur. J. Inorg. Chem.*, 2006, 1976–1986.
39 L. M. P. Lima, R. Delgado, M. G. B. Drew, P. Brandao and V. Felix, *Dalton Trans.*, 2008, 6593–6608.
40 L. Gano, F. Marques, M. P. Campello, M. Balbina, S. Lacerda and I. Santos, *Q. J. Nucl. Med. Mol. Imaging*, 2007, **51**, 6–15.
41 I. Svobodová, J. Havlíčková, J. Plutnar, P. Lubal, J. Kotek and P. Hermann, *Eur. J. Inorg. Chem.*, 2009, **2009**, 3577–3592.
42 J. Havlíčková, H. Medová, T. Vitha, J. Kotek, I. Císařová and P. Hermann, *Dalton Trans.*, 2008, 5378–5386.
43 G. Giambastiani, W. Oberhauser, C. Bianchini, F. Laschi, L. Sorace, P. Brueggeller, R. Gutmann, A. Orlandini and F. Vizza, *Eur. J. Inorg. Chem.*, 2005, 2027–2031.
44 A. D. Sherry, *J. Alloys Compd.*, 1997, **249**, 153–157.
45 I. Svobodová, P. Lubal, P. Hermann, J. Kotek and J. Havel, *Microchim. Acta*, 2004, **148**, 21–26.
46 I. Svobodová, P. Lubal, P. Hermann, J. Kotek and J. Havel, *J. Inclusion Phenom. Macrocyclic Chem.*, 2004, **49**, 11–15.
47 I. Lukeš, J. Kotek, P. Vojtíšek and P. Hermann, *Coord. Chem. Rev.*, 2001, **216**, 287–312.
48 X. K. Sun, M. Wuest, Z. Kovacs, A. D. Sherry, R. Motekaitis, Z. Wang, A. E. Martell, M. J. Welch and C. J. Anderson, *JBIC, J. Biol. Inorg. Chem.*, 2003, **8**, 217–225.
49 H. A. Fleisch, R. G. G. Russell, S. Bisaz, R. C. Mühlbauer and D. A. Williams, *Eur. J. Clin. Invest.*, 1970, **1**, 12–18.
50 R. G. G. Russell, R. C. Mühlbauer, S. Bisaz, D. A. Williams and H. Fleisch, *Calcif. Tissue Res.*, 1970, **6**, 183–196.
51 A. Zieba, G. Sethuraman, F. Perez, G. H. Nancollas and D. Cameron, *Langmuir*, 1996, **12**, 2853–2858.
52 Z. Amjad, *Langmuir*, 1987, **3**, 1063–1069.
53 C. A. Boswell, C. A. S. Regino, K. E. Baidoo, K. J. Wong, D. E. Milenic, J. A. Kelley, C. C. Lai and M. W. Brechbiel, *Bioorg. Med. Chem.*, 2009, **17**, 548–552.

54 J. Plutnar, J. Havlickova, J. Kotek, P. Hermann and I. Lukes, *New J. Chem.*, 2008, **32**, 496–504.
55 D. J. Stigers, R. Ferdani, G. R. Weisman, E. H. Wong, C. J. Anderson, J. A. Golen, C. Moore and A. L. Rheingold, *Dalton Trans.*, 2010, **39**, 1699–1701.
56 C. J. Anderson and R. Ferdani, *Cancer Biother. Radiopharm.*, 2009, **24**, 379–393.
57 P. Kafarski and J. Zon, in *Aminophosphonic Aminophosphinic Acids*, ed. V. P. Kukhar and H. R. Hudson, John Wiley & Sons, Ltd, Chichester, 2000, ch. 2, pp. 33–74.
58 M. Syamala, *Org. Prep. Proced. Int.*, 2005, **37**, 103–171.
59 S. Bhagat and A. K. Chakraborti, *J. Org. Chem.*, 2007, **72**, 1263–1270.
60 N. S. Zefirov and E. D. Matveeva, *ARKIVOC*, 2008, **1**, 1–17.
61 R. A. Cherkasov and V. I. Galkin, *Russ. Chem. Rev.*, 1998, **67**, 857–882.
62 G. Weisman, M. Rogers, E. Wong, J. Jasinski and E. Paight, *J. Am. Chem. Soc.*, 1990, **112**, 8604–8605.
63 J. Dale, *Acta Chem. Scand.*, 1973, **27**, 1115–1129.
64 J. Dale, in *Topics in Stereochemistry*, ed. N. L. Allinger and E. L. Eliel, John Wiley & Sons, New York, 1976, vol. 9, pp. 199–270.
65 K. J. Heroux, K. S. Woodin, D. J. Tranchemontagne, P. C. B. Widger, E. Southwick, E. H. Wong, G. R. Weisman, S. A. Tomellini, T. J. Wadas, C. J. Anderson, S. Kassel, J. A. Golen and A. L. Rheingold, *Dalton Trans.*, 2007, 2150–2162.
66 T. Hubin, N. Alcock and D. Busch, *Acta Crystallogr., Sect. C: Cryst. Struct. Commun.*, 2000, **C56**, 37–39.
67 T. Hubin, J. McCormick, N. Alcock, H. Clase and D. Busch, *Inorg. Chem.*, 1999, **38**, 4435–4446.
68 G. R. Weisman, E. H. Wong, D. C. Hill, M. E. Rogers, D. P. Reed and J. C. Calabrese, *Chem. Commun.*, 1996, 947–948.
69 W. Niu, E. Wong, G. Weisman, L. Zakharov, C. Incarvito and A. Rheingold, *Polyhedron*, 2004, **23**, 1019–1025.
70 A. Becke, *J. Chem. Phys.*, 1993, **98**, 5648.
71 C. Lee, W. Yang and R. G. Parr, *Phys. Rev. B*, 1988, **37**, 785.
72 P. J. Stephens, F. J. Devlin, C. F. Chabalowski and M. J. Frisch, *J. Phys. Chem.*, 1994, **98**, 11623–11627.
73 S. H. Vosko, L. Wilk and M. Nusair, *Can. J. Phys.*, 1980, **58**, 1200–1211.
74 J. Tirado-Rives and W. L. Jorgensen, *J. Chem. Theory Comput.*, 2008, **4**, 297–306.
75 Y. Zhao and D. G. Truhlar, *Acc. Chem. Res.*, 2008, **41**, 157–167.
76 Y. Zhao and D. G. Truhlar, *Theor. Chem. Acc.*, 2008, **120**, 215–241.
77 C. J. Cramer and D. G. Truhlar, *Phys. Chem. Chem. Phys.*, 2009, **11**, 10757.
78 T. M. Jones-Wilson, K. A. Deal, C. J. Anderson, D. W. McCarthy, Z. Kovacs, R. J. Motekaitis, A. D. Sherry, A. E. Martell and M. J. Welch, *Nucl. Med. Biol.*, 1998, **25**, 523–530.
79 Y. Guo, R. Ferdani and C. J. Anderson, *J. Lab. Comp. Radiopharm.*, 2011, **54 suppl 1**, S368.
80 M. Fani, L. Del Pozzo, K. Abiraj, R. Mansi, M. Tamma, R. Cescato, B. Waser, W. Weber, J. Reubi and H. Maecke, *J. Nucl. Med.*, 2011, **52**, 1110–1118.
81 R. A. Dumont, F. Deininger, R. Haubner, H. R. Maecke, W. A. Weber and M. Fani, *J. Nucl. Med.*, 2011, **52**, 1276–1284.
82 N. M. Di Bartolo, A. M. Sargeson, T. M. Donlevy and S. V. Smith, *J. Chem. Soc., Dalton Trans.*, 2001, 2303–2309.
83 G. A. Bottomley, I. J. Clark, I. I. Creaser, L. M. Engelhardt, R. J. Geue, K. S. Hagen, J. M. Harrowfield, G. A. Lawrance, P. A. Lay, A. M. Sargeson, A. J. See, B. W. Skelton, A. H. White and F. R. Wilner, *Aust. J. Chem.*, 1994, **47**, 143–179.
84 R. J. Geue, T. W. Hambley, J. M. Harrowfield, A. M. Sargeson and M. R. Snow, *J. Am. Chem. Soc.*, 1984, **106**, 5478–5488.
85 K. Wieghardt, U. Bossek, P. Chaudhuri, W. Herrmann, B. C. Menke and J. Weiss, *Inorg. Chem.*, 1982, **21**, 4308–4314.
86 C. A. Boswell, P. McQuade, G. R. Weisman, E. H. Wong and C. J. Anderson, *Nucl. Med. Biol.*, 2005, **32**, 29–38.
87 Y. Shao, L. F. Molnar, Y. Jung, J. Kussmann, C. Ochsenfeld, S. T. Brown, A. T. B. Gilbert, L. V. Slipchenko, S. V. Levchenko, D. P. O'Neill, R. A. DiStasio Jr, R. C. Lochan, T. Wang, G. J. O. Beran, N. A. Besley, J. M. Herbert, C. Yeh Lin, T. Van Voorhis, S. Hung Chien, A. Sodt, R. P. Steele, V. A. Rassolov, P. E. Maslen, P. P. Korambath, R. D. Adamson, B. Austin, J. Baker, E. F. C. Byrd, H. Dachsel, R. J. Doerksen, A. Dreuw, B. D. Dunietz, A. D. Dutoi, T. R. Furlani, S. R. Gwaltney, A. Heyden, S. Hirata, C.-P. Hsu, G. Kedziora, R. Z. Khalliulin, P. Klunzinger, A. M. Lee, M. S. Lee, W. Liang, I. Lotan, N. Nair, B. Peters, E. I. Proynov, P. A. Pieniazek, Y. Min Rhee, J. Ritchie, E. Rosta, C. David Sherrill, A. C. Simmonett, J. E. Subotnik, H. Lee, Woodcock Iii, W. Zhang, A. T. Bell, A. K. Chakraborty, D. M. Chipman, F. J. Keil, A. Warshel, W. J. Hehre, H. F. Schaefer Iii, J. Kong, A. I. Krylov, P. M. W. Gill and M. Head-Gordon, *Phys. Chem. Chem. Phys.*, 2006, **8**, 3172–3191.